Australian Journal of Basic and Applied Sciences, 6(6): 382-391, 2012
ISSN 1991-8178

Polyamide Thin Film Composite Membranes Using Interfacial Polymerization: Synthesis, Characterization and Reverse Osmosis Performance for Water Desalination

Abdel-hameed Mostafa A. El-Aassar

Desalination unit, Hydrogeochemistry Department, Desert Research Center (DRC), Cairo, Egypt.

Abstract: A variety of polyamide thin film composite (PA-TFC) membranes was synthesized via interfacial polymerization (IP) technique. IP was carried out between aqueous solution of *m*-phenylene diamine (MPD) and trimesoyl chloride (TMC) in dodecane as organic solvent onto polysulfone (PSf) supporting membrane. The characterization of synthesized membranes was conducted using attenuated total reflection Fouier transform infrared spectroscopy (ATR-FTIR), scanning electron microscope (SEM) and contact angle measurement. Reverse osmosis performance included permeate flux (L/m^2.hr) and salt rejection (%) was evaluated as a function of the synthesis conditions to investigate the optimum conditions that give the best performance membrane. The optimum conditions of synthesized membranes included MPD (1.5 wt.%) for 5 min. soaking time, TMC (0.05 wt. %) in dodecane for 30 sec. reaction time. The best synthesized membrane exhibited high salt rejection (99.81%) with high permeate flux (36.15 L/m^2.h). Also, the concentration polarization modulus (*M*) and the true salt rejection (%) were measured using pure water with different salinities up to ≈ 10000 ppm NaCl feed solution. The obtained results showed that the concentration polarization modulus (*M*) ranged from 1.06 to 1.29 according to the sanity range.

Key words: *Polyamide; thin-film composite; interfacial polymerization; characterization; reverse osmosis performance.*

INTRODUCTION

In the 21st century, the most crucial problem afflicting people around the world is global water scarcity. The rapid growth in population and economy have resulted in greater demand on the quantity and quality of drinking water, leading to catastrophic water shortage in arid and water-stressed regions (Shannon *et al.,* 2008). It is projected that by the year 2030, the global needs of water would increase to 6900 billion m^3 from the current 4500 billion m^3 (2030 Water resources group 2009). As a result, the present water resources will no longer be sufficient to meet the future needs for mankind. With the fact that only around 0.8% of the total earth's water is fresh water (Greenlee *et al.,* 2009), numerous researches were conducted in an effort to develop more sustainable technological solutions that would meet increasing water consumption. Of the technologies developed, desalting seawater to produce clean water for drinking, irrigation, industrial and urban development emerged as the most sustainable approach (Uemura and Henmi 2008). In general, desalination technologies can be categorized into two different mechanism separations, i.e. thermal and membrane-based desalination. The thermal processes include multi-stage flash (MSF), multiple effect distillation (MED) and vapor compression distillation (VCD), whereas membrane-based processes include reverse osmosis (RO), nanofiltration (NF) and electrodialysis (ED). Among these technologies, RO membrane desalination is the primary choice where it dominates up to 44% of the total world desalination capacity (Greenlee *et al.,* 2009).

Thin film composite (TFC) membranes are extensively used in reverse osmosis (RO) desalination applications. Since the breakthrough discovery made by Cadotte and his co-workers in the 1970s, thin-film composite (TFC) membrane, prepared using interfacial polymerization (IP) technique, has experienced significant progress in composite membrane development and emerged as one of the most advanced technologies in water and wastewater purification processes (Misdan *et al.,* 2012).

These membranes have a thin and dense active layer that controls membrane performance (permeability and selectivity), and a much thicker porous substrate that provides mechanical support to the active layer. In order to achieve high values of permeability and selectivity, the active layer should be ultrathin and hydrophilic. A variety of polymers and formation schemes have been employed for this purpose (Kesting 1990; Kimmerle and Strathmann 1990). Overall, polyamide structures fabricated via (IP) have provided the most successful RO membranes (Sundet *et al.,* 1987; Cheng *et al.,* 1991; Desai *et al.,* 1992). The ultra-thin polyamide films synthesized via (IP) can exhibit a range of physicochemical properties based on the polymerization conditions including the monomer concentration and the reactant ratio (Morgan 1965; Chai and Krantz 1994). These properties play a pivotal role in membrane performance. For the current studies, PA-TFC membranes were synthesized using *m*-phenylenediamine (MPD) and trimesoyl chloride (TMC) on a polysulfone support via IP (Rozelle *et al.,* 1977; Cadotte 1981). As indicated in Fig. 1, the polyamide contains a crosslinked portion (X) and a more hydrophilic linear moiety (Y) containing free carboxylic acid groups (Roh *et al*., 2006). The number

Corresponding Author: Abdel-hameed Mostafa A. El-Aassar, Desalination unit, Hydrogeochemistry Department, Desert Research Center (DRC), Cairo, Egypt.

of free carboxylic acid groups as well as the thickness and mechanical properties of the thin film are governed by the monomer concentrations and the NH_2/COCl molar ratio. The permeate flux of RO membranes is reported to be influenced by hydrophilicity, thickness and density of the polyamide barrier layer (Petersen 1993, Morgan 1965).

Generally, interfacial polymerization of MPD and TMC is believed to involve an incipient fast stage that forms a dense core barrier layer followed by a slow growth stage that is MPD diffusion limited (Chai and Krantz 1994, Song *et al.,* 2005). The fast reaction in the incipient stage provides the dense core layer that is significantly thinner than the extended loose layer formed later as monomer diffuses through the dense core layer (Freger 2005). The thickness of the dense core layer decreases as the concentration of either monomer increases. Also, the flux and rejection depend on the PA barrier layer crosslinked density (Song *et al.,* 2005).The core layer is the most dense region, and the polymer density decreases gradually as the polymer grows further into the organic phase (Freger 2003; Pacheco *et al.,* 2010; Berezkin and Khokhlov 2006).

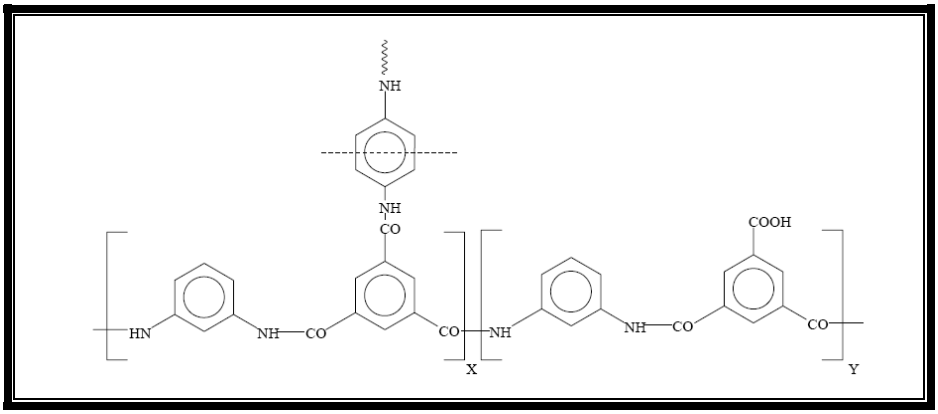

Fig. 1: The polyamide structure formed from an IP reaction between MPD and TMC has a crosslinked portion (X-fraction) and linear moiety (Y-fraction), which has an un-reacted acid chloride group that subsequently, hydrolyzes to a carboxylic acid group.

Consequently, the aim of this study was to evaluate the effect of synthesis conditions such as MPD concentration in the aqueous solution, MPD soaking time, TMC concentration in dodecane solution and the reaction time on the obtained PA active layer properties which affects on the membrane performance. It provides a description of the relationships among the composition, properties and performance of PA-TFC membranes, and yields useful insights regarding the means by which membrane performance can be optimized. The influence of salt polarization on apparent rejection was estimated using best synthesized TFC membrane using pure water and different feed water salinity to evaluate the synthesized PA-TFC membrane performance in a wide salinity range and calculate both the concentration polarization modulus (*M*) and the true salt rejection (%).

2. Experimental:

2.1. Materials and Reagents:

Asymmetric polysulfone (PSf) support membrane on non-woven polyester fabric was kindly supplied by Dow Water & Process Solutions (Edina, MN). *m*-phenylenediamine (MPD, ≥ 99%), trimesoyl chloride (TMC, 98%), triethylamine (TEA, ≥ 99%), *n*-dodecane (anhydrous, ≥ 99%) and *n*-hexane (mixture of isomers, anhydrous,≥ 99%) were used as received from Sigma-Aldrich (St. Louis, MO). Deionized (DI) water was generated by a Milli-Q Advantage A10 vacuum purification system (Millipore, Billerica, MA).

Acrylic plastic plates with dimensions (8 in x 11 in x 0.24 in) were used to support PSf membranes during TFC membranes preparation. Additionally, plastic frames (inner size: 6 in x 9 in) were cut from these plates. Rubber gaskets having the same size of the plastic frames were purchased from Advanced Gasket & Supply (Fort Worth, TX, USA). Soft rubber rollers were purchased from Sigma-Aldrich Co. (St. Louis, MO, USA).

2.2. Preparation of Polyamide Thin-Film (PA-TFC) Membranes:

The process of membrane preparation is similar to that reported by Mitchell *et al.,* 2011 and Xie *et al.,* 2012, as shown in Fig.(2).

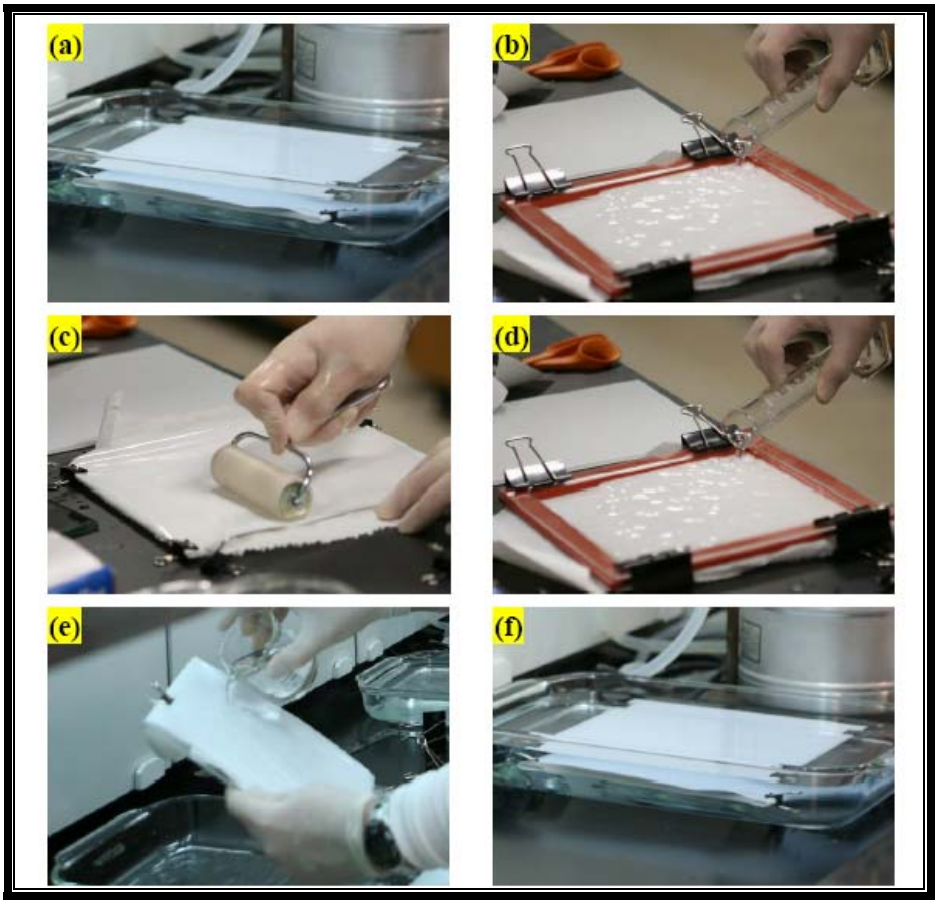

Fig. 2: Protocol to prepare polyamide TFC membranes, Xie *et al.*, 2012.

PSf support membranes were immersed in DI water for one hour, (Fig.2-a) then removed from water and positioned on a plastic plate. A rubber gasket and a plastic frame were placed on top of the support membrane, and binder clips were used to hold the plate-membrane-gasket-frame stack together. MPD aqueous solution was poured into the frame (Fig.2-b) and allowed to contact the PSf membrane for a time before draining the excess MPD solution. This residence time allowed MPD to penetrate into the pores of the porous PSf support layer.

The frame and gasket were disassembled and residual solution between the plate and the PSf was removed. Residual droplets of MPD aqueous solution on the top surface of the PS membrane were removed by rolling a rubber roller across the membrane surface (Fig.2-c) to ensure no visible aqueous droplets, which could form defects if left on the membrane surface. The frame and gasket were reassembled on top of the membrane, and TMC in organic solution was poured into the frame (Fig.2-d). After a time, the organic solution was drained from the frame, and the frame and gasket were disassembled. TFC membrane surface was washed by hexane (Fig.2-e) and let to dry in air at ambient conditions. Finally the prepared membrane was immersed in DI water (Fig.2-f) until characterized or used in cross flow experiments.

2.3. Characterization of Polyamide Thin-Film (PA-TFC) Membranes:

The chemical structure of PA-TFC membranes was characterized using attenuated total reflectance Fourier transform infrared spectroscopy (ATR-FTIR). A Thermo Nicolet Nexus 470 FTIR with an Avatar Smart Miracle ATR accessory and a ZnSe crystal (Thermo Fisher Scientific Inc., Waltham, MA) was used. Spectra were collected in air, in the mid-infrared region (600-4000 cm^{-1}), using 128 scans at resolution 4. After each measurement, a background spectrum was obtained using PSf membrane and subtracted from that of the membrane to remove any atmospheric absorbance peaks.

Also, membrane surface and cross-section morphology was characterized by scanning electron microscopy (SEM, Zeiss Supra 40 VP, Carl Zeiss NTS, Peabody, MA). High voltage ETH mode was used and the voltage was set to 5 kv. An In Lens detector was selected, and the working distance was between 5 and 7 mm. Samples were prepared by peeling away the no-woven polyester backing fabric and fracturing the remaining polysulfone and polyamide layers after immersion in liquid nitrogen. A Cressington 208 Bench-top Sputter Coater

(Cressington Scientific Instruments LTD., Watford, England) having a Pt/Pd metal target was used to coat the samples. The coating thickness was set at 10 nm to ensure adequate sample surface conductivity.

The membrane hydrophilicity was evaluated through contact angle measurement. The Oil-in-water contact angle analysis was performed using a Ramé-Hart Model 200-F1 Standard Goniometer with DROP image Standard Edition 2.4 software (Ramé-Hart Instrument Co., Netcong, NJ). A strip of membrane was mounted in a sample holder with active side facing down and placed in DI water environment. An n-decane oil droplet was dispensed onto the bottom side of the membrane strip from a Gilmont Instruments 0.2 ml micrometer syringe (Cole-Parmer Instrument Co., Vernon Hills, IL) with a hooked Hamilton N732 needle (OD: 0.009 in, Hamilton Co., Reno, NV). Contact angles were measured through the water phase, and the reported contact angle is the average value of the left and right side contact angles, at least three oil droplets were placed at different spots in each sample (any membrane was measured using 3 samples). A smaller angle indicates a more hydrophilic surface.

2.4. Reverse Osmosis Performance of Polyamide Thin-Film (PA-TFC) Membranes:

The reverse osmosis performance of the prepared PA-TFC membranes was evaluated through measuring both permeate flux ($L/m^2.h$) and salt rejection (%). Permeate flux and salt rejection were measured using crossflow filtration and aqueous feed solution containing 2000 ppm NaCl with pH range 7± 0.2 at 25°C. The flow rate was 1g/min and the applied pressure was 225 psi (15.5 bar). All flux and rejection measurements were evaluated after 30 min from the start of crossflow experiment to ensure that the filtration process had reached steady state.

The permeate flux (J_W) through a membrane area (A) was calculated as the volume (ΔV) collected during a time period Δt:

$$J_W = \Delta V / A . \Delta t$$

Also, the salt rejection (R_s %) was calculated by measuring the electric conductivity of both feed and permeate solutions using an Oakton CON 11 conductivity meter (cole-Parmer Instrument Co., Vernon Hills, IL) and calculated as follows:

$$R_s\% = (C_f - C_p/C_f) \times 100$$

Where C_f and C_p are the concentrations of the feed and permeate water (product), respectively.

RESULTS AND DISCUSSION

3.1. Synthesis and Characterization of PA-TFC Membranes:

In order to investigate the optimum synthesis conditions of PA-TFC membranes, the effect of different parameters that expected to influence the IP reaction and obtained membrane performance were studied through four series of IP reactions, as shown in Table (1).

Table 1: Summary of the reaction conditions for the synthesized PA-TFC membranes.

Series	MPD conc. (wt. %)	Soaking time (min.)	TMC conc. (wt. %)	Reaction time (sec.)
I	0.5-2.5	5	0.05	60
II	1.5	1-10	0.05	60
III	1.5	5	0.01-0.1	60
IV	1.5	5	0.05	15-120

The chemical composition of both PSf support layer and synthesized PA-TFC membrane surface was investigated by ATR-FTIR, (Fig. 3). The spectrum of the PSf membrane (Fig. 3a), shows peaks at 1587- 1487, 1324, 1294, 1235, 1150-1106cm^{-1} assigned to C-C, C-H, O=S=O (symmetric), C-O-C and O=S=O (asymmetric), respectively. Because the depth of ATR-RTIR penetration was about 0.4-0.5 µm in the wavelength region of interest (Xie *et al.,* 2012), the spectra reflect a combination of polyamide barrier layer (0.1-0.15 µm) and the rest of PSf substrate. The spectra of PA-TFC membrane (fig. 3b) show the absence of the acid chloride band at 1770cm^{-1}, indicating that successful polymerization has occurred. The bands at 1661 and 1549 cm^{-1} were present, that is characteristic of (amide I) C=O stretching vibrations and amide-II (N–H) band of amide group (–CONH–). In addition, other bands characteristic of PA occur at 1609.6 and 1488.9cm^{-1} (aromatic ring breathing), and 1250 cm^{-1} (amide III). Also, the stretching peak of OH group was present at 3384 cm^{-1}.

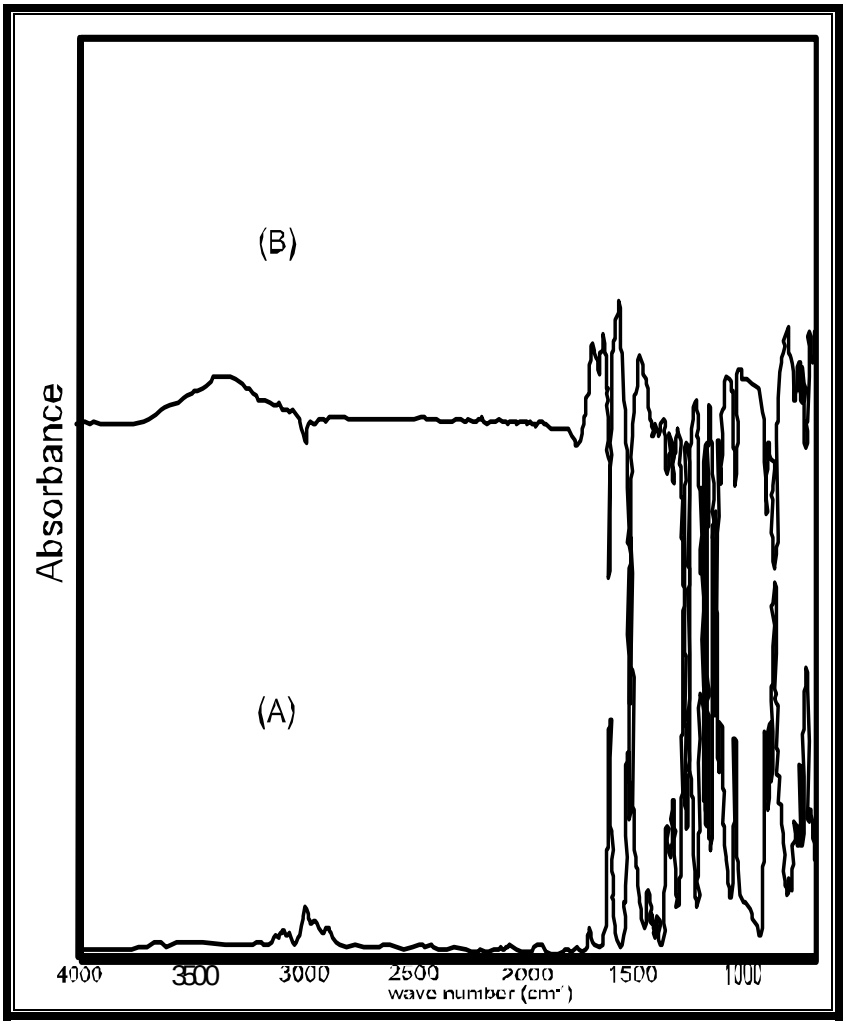

Fig. 3: ATR-FTIR of (A) PS support layer and (B) PA-TFC membrane.

Also, the membrane surfaces and cross sections were imaged by SEM as seen in Figure (4). PSf porous layer possesses smooth surface while the synthesized polyamide TFC surface had a tightly packed globules and scattered ear-shaped polyamide ridges, presumably generated on top of the polysulfone support layer having surface pores so that MPD could diffuse into the organic phase to form these micro-protuberances.

The surface hydrophilicity is evaluated through contact angle measurements of all membranes, as shown in tables (2-5). It is clear that the contact angle of all membranes ranged from 23.7º± 3 to 39.5º ± 2, this indicates the high hydrophilicity of the obtained PA-TFC membranes as compared to PSf support layer with 85ºcontact angle. The contact angle of the synthesized PA-TFC membranes decreased, i.e., the hydrophilicity increased, by increasing of concentration of TMC or decreasing of MPD concentration due to formation of linear portion of PA which possesses free –COOH groups.

3.2. Performance Optimization of TFC Reverse Osmosis Membranes:

In general, the performance of the composite membrane is determined by the chemistry and the preparation conditions of the ultra-thin selective layer. So, in the study, the effect of preparation parameters was studied to obtain an optimized set of conditions for the development of PA-TFC membrane with best RO performance.

3.2.1. Effect of MPD Monomer Concentration:

The influence of MPD monomer concentration on both salt rejection (%) and permeate flux ($L/m^2.hr$) was illustrated in table (2).

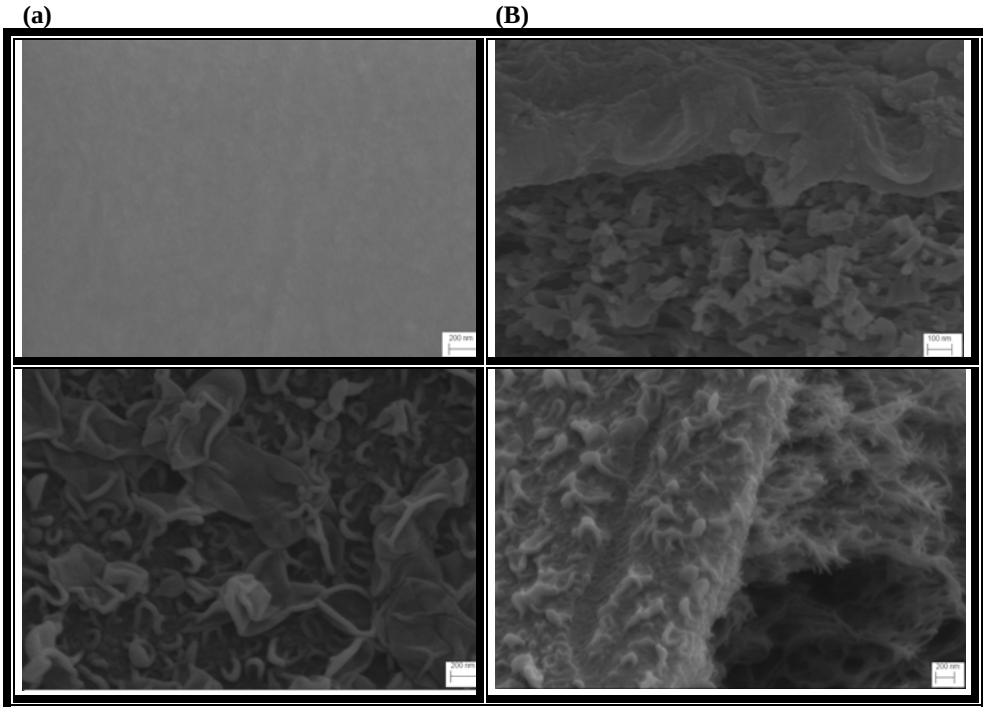

Fig. 4: SEM images of polysulfone (upper) and PA-TFC membranes (lower); for both top surfaces (a) and cross sections (b).

Table 2: Effect of MPD monomer concentration on both salt rejection and permeate flux, series I: soaking time (5min.), TMC (0.05wt %), reaction time (1min.).

MPD Conc. (wt.%)	Salt Rejection (%)	Permeate Flux (L/m^2.h)	NH_2/COCl Molar ratio	Contact angle
0.5	99.4	14.97	16.37	23.7± 3
1	99.81	27.21	32.75	27.2± 3
1.5	99.81	35.11	49.12	28.2± 2
2	99.8	33.65	65.5	28.9± 3
2.5	99.8	31.72	81.87	35.9± 2

All synthesized membranes have high salt rejection that ranged from 99.4 to 99.81%, suggesting the formation of defect free PA layer in all cases. It is obvious that, the salt rejection increased by increasing the MPD concentration up to 1wt. %, then it became relatively insensitive to MPD concentration over the range of concentration considered (1-2.5wt.%). The permeate flux exhibited the maximum value at 1.5wt.% of MPD concentration which gave the optimum molar ratio, at which fast formation of a dense PA barrier layer takes place due to the presence of a large number of MPD monomer at the vicinity of the interface, and the film is expected to be thinner and more homogenous. Further increase of MPD concentration increases the driving force for diffusion of MPD into the organic phase, thereby increasing the polyamide thickness during the slow growth stage, so the flux will decrease. On the other hand, a low concentration of MPD leads to decreasing the molar ratio which becomes closer to unity and form thicker and looser PA barrier layer which decreases both permeate flux and salt rejection (Song *et al.,* 2005).

3.2.2. Effect of MPD Soaking Time:

Also, the effect of MPD soaking time on both salt rejection and permeate flux was studied as shown in table (3).

It is clear that both salt rejection (%) and permeate flux increased with increasing the MPD soaking time from 1 to 5 min., this is due to that as the soaking time increases the amount of MPD penetrates into PSf support layer pores increases. From table (3), the optimum soaking time is 5 min., after that both salt rejection and permeate flux was almost constant. So MPD soaking time was set at 5 minutes in all synthesized membranes reported hereafter.

Table 3: Effect of MPD soaking time on both salt rejection and permeate flux; series II: MPD (1.5wt. %), TMC (0.05wt %), reaction time (1min.).

MPD soaking Time (min.)	Salt Rejection (%)	Flux ($L/m^2.h$)	Contact angle
1	99.73	24.92	32.6± 4
2	99.76	27.15	28.5± 3
5	99.81	35.11	28.2± 2
10	99. 8	35.39	28.9± 2

3.2.3. Effect of TMC Monomer Concentration:

Table (4) shows the relationship between the TMC monomer concentration and both permeate flux and salt rejection (%). The table shows that, at very low TMC concentration (0.01 wt.%), low values of both salt rejection and water flux were obtained, this is due to the formation of less hydrophilic, loose and thick PA layer. By increasing the TMC concentration up to 0.05 wt. %, the reverse osmosis performance improved, i.e., improved both salt rejection and permeate flux, suggesting the formation of thinner, denser and more hydrophilic layer. The very high concentration (0.1 wt.%) leads to decreasing the molar ratio which becomes closer to unity and forms thicker PA barrier layer which decreases permeate flux.

Table 4: Effect of TMC monomer concentration on both salt rejection and permeate flux, series III: MPD conc. (1.5wt. %), soaking time (5min.), reaction time (1min.).

TMC Conc. (wt.%)	Salt Rejection (%)	Permeate Flux ($L/m^2.h$)	$NH_2/COCl$ Molar ratio	Contact angle (º)
0.01	93.25	29.76	245.6	35± 3
0.025	99.80	30.41	98.25	30.7± 2
0.05	99.81	35.11	49.12	28.2± 2
0.1	99.84	20.11	24.56	27.8± 2

3.2.4. Effect of Reaction Time:

It is well known that the interfacial polymerization between diamine and acid chloride occurs in the organic side, the reaction is diffusion-controlled and exists in a self-limiting phenomenon. The reaction time plays an important role in determining the extent of polymerization, and thereby the cross-linking degree and thickness of top skin layer as well as the resulting membrane performance (Morgan and Kwolek 1996; Ahmad and Ooi 2005). The top skin layer thickness of the composite membrane increases with increasing the polymerization time, and when the thin layer is thick enough to prevent diamine diffusing from aqueous phase into the organic phase, the top layer thickness will stop growing. As shown in table (5), for shorter reaction time (15 sec.), both salt rejection and water flux were low, this is due to the formation of less hydrophilic and loose skin layer with low degree of cross-linking which allow permeation of both water and salt, so both flux and salt rejection (%) were low. As the reaction time increases (30 sec.), the hydrophilicity and cross-linking degree of the polyamide skin layer will increase, this results in an increase of both salt rejection and permeate flux. Further increase of the reaction time (30-120 sec.), increases the PA layer thickness and the salt rejection with decreasing flux. The best reaction time of 30 sec. was selected.

Table 5: Effect of reaction time (sec.) on both salt rejection and permeate flux, series IV: MPD conc. (1.5wt. %), soaking time (5min.), TMC conc. (0.05 wt. %).

Reaction Time (sec.)	Salt Rejection (%)	Flux ($L/m^2.h$)	Contact angle
15	99.61	34.21	39.5± 2
30	99.81	36.15	28.2± 2
60	99.83	35.11	28.2± 2
120	99.86	34.86	32.5± 3

By comparing the results of different parameters that influenced the performance of synthesized membranes as mentioned before, the optimum condition of PA-TFC membranes was delineated. It includes 1.5 wt. % MPD for 5 min. soaking time and 0.05 wt. % for 30 sec. reaction time. The obtained membrane possesses high salt rejection (99.81%) with high water flux (36.15 L/ m^2.hr) and was selected as the best membrane.

3.3. Effect of Concentration Polarization and Feed Solution Salinity:

The high salt rejection coupled high permeate flux of any RO membranes contributes to concentration polarization, i.e., the salt concentration at the membrane surface is greater than the bulk feed concentration. This is due to accumulation of rejected salt in a boundary layer at the membrane surface. Since bulk feed concentration is typically used to calculate the apparent (measured) salt rejection, concentration polarization causes this apparent rejection value to be lower than the true rejection of the membrane. The true salt rejection can be calculated by measuring the salt concentration on the membrane surface using the model of the previous work (Sutzkover *et al*., 2000). At which, the permeate flux using both pure and saline water as well as the

concentrations of permeate and feed water were measured using the following equations (Eqs.1-3) (Baker 2004):

$$J_{w\,(PW)} = A_w . \Delta P \qquad \text{Eq.1}$$

Where; $J_{w\,(PW)}$ is the permeate flux when the feed solution is pure water, A_w is the effective membrane permeance to water and ΔP is the pressure difference across the membrane, at pure water $\Delta\Pi=0$.
Addition of NaCl salt to the feed reduces the permeate flux as follows:

$$J_{w\,(NaCl)} = A_w . (\Delta P - \Delta\Pi), \quad \Delta\Pi = \Pi_f^m - \Pi_P \qquad \text{Eq.2}$$

Where; $J_{w\,(NaCl)}$ is the permeate flux when the feed contains salt, Π_P is the permeate osmotic pressure, and Π_f^m is the osmotic pressure at the membrane surface on the feed side. The osmotic pressure is estimated as follows:

$$\Pi_i = C_i R_{gas} T \qquad \text{Eq. 3}$$

Where; Π_i is the osmotic pressure, C_i is the ion (i) concentration in solution, R_{gas} is the gas constant and T is the absolute temperature.

If A_w is constant, we get the following equation (Eq. 4) which may be used to calculate the actual salt concentration at the membrane surface.

$$\Pi_f^m = \Pi_P + \Delta P \times [1 - J_{w\,(NaCl)} / J_{w\,(PW)}] \qquad \text{Eq.4}$$

So we can calculate the true salt rejection using the following equation (Eq.5) [29].

$$R_s\,(true) = [C_f^m - C_p / C_f^m] \times 100 \qquad \text{Eq. 5}$$

Also, the concentration polarization modulus, *M*, which is defined as the ratio of the concentration difference between the feed solution at the membrane surface and the permeate solution to that between the bulk feed solution and the permeate solution as following equation (Eq. 6)

$$M = C_f^m - C_p / C_f - C_p \qquad \text{Eq. 6}$$

For the best selected membrane, reverse osmosis properties were measured using pure water and different salinities feed water to measure the true salt rejection at different salinities and concentration polarization (*M*) modulus, as shown in table (6). The operation condition included 225 psi (15.5 bar) applied pressure at 25ºC.

Table 6: Effect of feed water salinity on RO performance of the selected membranes.

Feed water salinity (ppm)	J_{H2O} (L/ m^2.hr)	Apparent R_S (%)	True R_S (%)	*M* Modulus
Pure water	41	-	-	-
2043	36.15	99.81	99.82	1.06
5525	26	99.5	99.59	1.22
9990	12.5	98.8	99.07	1.29

From the table, it is clear that, both flux and salt rejection (%) decrease with the increase of feed water concentration. On the other hand, the concentration polarization modulus (*M*) increases from 1.06-1.29 by increasing the feed water salinity from 2043 to 9990 ppm.

The decrease in permeate flux (J_{H_2O}) with increasing the feed water concentration can be explained as, the water flux through the membrane is proportional to the effective pressure (P_{eff}), which can be defined as:

$$P_{eff} \alpha P - \Delta\Pi$$

Where; P_{eff} and P are the effective and applied pressures and $\Delta\Pi$ is the osmotic pressure. The increase of the feed concentration at constant applied pressure leads to an increase in its osmotic pressure. Thus, the decrease in the effective pressure leads to a decrease in water flux.

In case of salt rejection, the decrease of salt rejection by increasing the feed concentration can be explained as mentioned in the previous works (Bartles *et al.,* 2005; McCurley and Seitz 1991; Flory 1953; Wong *et al.,* 2012), the passage of salt through the membrane in terms of several interacting mechanisms including convection, diffusion, and charge repulsion. Specifically, the combined influence of membrane charge and feed

ionic strength is known to play a significant role in salts rejection. Possible explanation for the observed trends is the swelling of the polymer in ionic solutions. The driving force for swelling is dependent on the difference between the charge density of the polymer and the ionic strength of the solution (McCurley and Seitz 1991). Therefore, at higher solution ionic strength, there is a greater ability of the solution to equalize the charge densities in the polymer, reducing electrostatic repulsion between polymer chains, and minimizing swelling (Flory 1953).

4. Conclusions:

Thin-film composite reverse osmosis membrane comprising the selective ultra-thin skin layer of aromatic polyamide was successfully synthesized from aqueous solution of *m*-phenylenediamine and trimesoyl chloride in dodecane solution through interfacial polymerization on porous polysulfone supporting film. The optimum conditions of PA-TFC synthesis were investigated through studying the different parameters that affect the synthesized membranes such as MPD, TMC concentrations, MPD soaking time and the reaction time. The optimum conditions include (1.5 wt. %) MPD concentration for 5 min. soaking time, (0.05 wt. %) TMC concentration with 30 sec. reaction time. The results from the reverse osmosis performance test indicated that the desired membrane prepared under the optimum condition exhibited high salt rejection (99.81%) with high permeate flux (36.15 L/ m^2.h).

The obtained results of permeate flux using pure water and different salinities revealed that the concentration polarization modulus (*M*) ranged from 1.06 to 1.29 according to the sanity range. The synthesized membranes possessed high true salt rejections with high permeate flux within a wide range of salinity and can be applicable for desalination of saline water.

ACKNOWLEDGEMENTS

The author expresses his thanks Science and Technology Development Fund (STDF) and USA-Egypt Science and Technology collaboration program for supporting his scientific visit to chemical Engineering Dept., Texas University at Austin, Texas, USA.

REFERENCES

Ahmad, A.L. and B.S. Ooi, 2005. “Properties–performance of thin film composites membrane: study on tri-mesoyl chloride content and polymerization time”, Journal of Membrane Science, 255: 67-77.

Baker, R.W., 2004. “Membrane Technology and Applications, 2nd ed.”, J. Wiley, Chichester.

Berezkin, A.V. and A.R. Khokhlov, 2006. “Mathematical modeling of interfacial polycondesation”, Journal of Polymer Science, B-Polym. Phys., 44: 2698-2724.

Cadotte, J.E., 1981. “Interfacially Synthesized Reverse Osmosis Membrane”, US Patent, 4: 277-344.

Chai, G.Y. and W.B. Krantz, 1994. “Formation and characterization of polyamide membranes via interfacial polymerization”, J. Membr. Sci., 93: 175-192.

Cheng, R., J. Glater, J.B. Neethling and M.K. Stenstrom, 1991. “The effects of small halocarbons on RO membrane performance”, Desalination, 85: 33.

Craig B., R. Franks, S. Rybar, M. Schierach, M. Wilf, 2005. “The effect of feed ionic strength on salt passage through reverse osmosis membranes”, Desalination, 184: 185-195.

Desai, N.V., R. Ranggarajan, A.V. Rao, D.K. Garg, B.V. Ankleschwaria and M.H. Mehta, 1992. “Preliminary investigation of thin film composite reverse osmosis membranes developed from SAN as support membranes”, Journal of Membrane Science, 71: 201.

Flory, P.J., 1953. “Principles of Polymer Chemistry”, Cornell University Press, Ithaca, NY.

Freger, V., 2003. “Nanoscale heterogeneity of polyamide membranes formed by interfacial polymerization”, Langmuir 19: 4791-4797.

Freger, V., 2005. “Kinetics of film formation by interfacial poly-condensation”, Langmuir 21: 1884-1894.

Freger, V. and S. Srebnik, 2003. “Mathematical model of charge and density distributions in interfacial polymerization of thin films”, J. Appl. Polym. Sci., 88: 1162-1169.

Greenlee, L.F., D.F. Lawler, B.D. Freeman, B. Marrot and P. Moulin, 2009. “Reverse osmosis desalination: water sources, technology, and today's challenges”, Water Res., 43: 2317-2348.

Kesting, R.E., 1990. “The four tiers of structure in integrally skinned phase inversion membranes and their relevance to the various separation regimes”, J. Appl. Polym. Sci., 41: 2739.

Kimmerle K. and H. Strathmann, 1990. “Analysis of the structure-determining process of phase inversion membranes”, Desalination, 79: 283.

McCurley, M.F. and W.R. Seitz, 1991. “Fiber-optic sensor for salt concentration based on polymer swelling coupled to optical displacement”, Anal. Chim. Acta, 249: 373-380.

Misdan N., W.J. Lau and A.F. Ismail, 2012. "Seawater Reverse Osmosis (SWRO) desalination by thin-film composite membrane-Current development, challenges and future prospects", Desalination, 287: 228–237

Mitchell, G.E., B. Mickols, D. Hernandez-Cruz and A. Hitchcock, 2011. "Unexpected new phase detected in FT30 type reverse osmosis membranes using scanning transmission X-ray microscopy", Polymer, 52: 3956-3962.

Morgan, P.W., 1965. "Condensation polymer by interfacial and solution methods", Inter science Publishers, New York, USA.

Morgan, P.W. and S.L. Kwolek, 1996. "Interfacial polymerization. 2. Fundamentals of polymer formation at liquid interface, J. Polym. Sci. Pt. A: Polym. Chem., 34: 531.

Pacheco, F. A., I. Pinnau, M. Reinhard and J. O. Leckie, 2010. "Characterization of isolated polyamide thin films of RO and NF membranes using novel TEM techniques", J. Membr. Sci., 358: 51-59.

Petersen, R.J., 1993. "Composite reverse-osmosis and Nanofiltration membranes", J. Membrane Sci., 83: 81-150.

Roh I. J., R.A. Greenberg and V.P. Khare, 2006. "Synthesis and characterization of interfacially polymerized polyamide thin films", Desalination, 191: 279-290.

Rozelle, L.T., J.E. Cadotte, K.E. Cobian, C.V. Kopp and S. Sourirajan, 1977. "NS-100 Membranes for Reverse Osmosis and Synthetic Membranes", National Research Council Canada, Ottawa, Canada, 1977, pp. 249.

Shannon, M.A., P.W. Bohn, M. Elimelech, J.G. Georgiadis, B.J. Marinas and A.M. Mayes, 2008. "Science and technology for water purification in the coming decades", Nature, 452: 301–310.

Song,Y. J., P. Sun, L. L. Henry and H. H. Sun, 2005. " Mechanisms of structure and performance controlled thin film composite membrane formation via interfacial polymerization process", J. Membr. Sci., 251: 67.

Sundet, S.A., S.D. Arthur, D. Campos, T.J. Eckman and R.G. Brown, 1987. "Aromatic/cycloaliphatic polyamide membrane", Desalination, 64: 259.

Sutzkover, I., D. Hasson, R. Semiat, 2000. "Simple technique for measuring the concentration polarization level in a reverse osmosis system", Desalination, 131: 117-127.

Uemura T. and M. Henmi, 2008. "Thin-film Composite Membranes for Reverse Osmosis", John Wiley & Sons, Inc.

Wong, M. C.Y., K. Martinez, G. Z. Ramon and E. M.V. Hoek, 2012. "Impacts of operating conditions and solution chemistry on osmotic membrane structure and performance", Desalination, 287: 340-349.

Xie, W., G. M. Geise, B. d. Freeman, H. Lee, G. Byun. and J. E. Mcgrath, 2012. "Polyamide interfacial composite membranes prepared from m-phenylene diamine, trimesoyl chloride and a new disulfonated diamine", Journal of Membrane Science, 403–404: 152-161.

2030 Water Resources Group, 2009. Charting our water future-economic frameworks to inform decision-making.